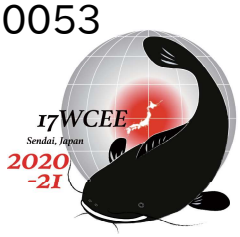

17th World Conference on Earthquake Engineering, 17WCEE
Sendai, Japan - September 27th to October 2nd, 2021

Incorporating Epistemic and Aleatory uncertainties in Fragility modelling of Masonry Structures in Portugal

H. Lovon[(1)], V. Silva[(2)], R. Vicente[(3)], T.M. Ferreira[(4)]

[(1)] *PhD student, RISCO Civil Engineering Department University of Aveiro, Portugal, holger.lovonq@ua.pt*
[(2)] *Professor, Universidade Fernando Pessoa, Portugal, vitor.silva@globalquakemodel.org*
[(3)] *Professor, Civil Engineering Department University of Aveiro, Portugal, romvic@ua.pt*
[(4)] *Researcher, ISISE Institute of Science and Innovation for Bio Sustainability (IB-S), tmferreira@civil.uminho.pt*

Abstract

The evaluation of the seismic vulnerability of existing structures for regional risk analysis is characterized by sources of uncertainty due to insufficient data (i.e. epistemic) and sources of variability that cannot be reduced (i.e. aleatory). These sources of uncertainty are particularly important for the evaluation of fragility of masonry structure, whose material and geometric properties can vary considerably even within structures of the same building class. This work investigates the impact of epistemic and aleatory uncertainties in the fragility modelling of masonry buildings, with an application to the Portuguese building stock. The geometrical features of the masonry building stock is considered by gathering information from a set of drawings, including the wall thickness, inter-story height, density of walls, among others. These statistics were used to generate a number of representative buildings, by sampling the geometric and material properties. The seismic demand was represented by a set of ground motion records to cover the span of intensity motions according to the seismic hazard of the zone of study. The structural response of the set of buildings was analysed using block-based FEM technique implemented in the LS-Dyna software. This tool allows modelling structural damage, including explicitly structural collapse. This approach allows assessing not just damage and economic losses, but also potential casualties due to fall of debris. The results of the aforementioned analysis were used to compute fragility curves for damage and fatalities. A set of sampled buildings are tested against each record allowing the analysis of building-to-building variability, and how neglecting them might bias the fragility results.

Keywords: uncertainties, fragility, masonry, Portugal, Ls-Dyna

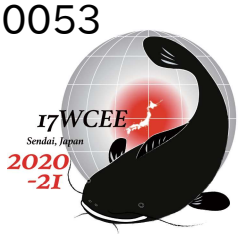

1. Introduction

In the past, deathly seismic events took place in Portugal such as ~M6.0 1722 Algarve, ~M8.5 1755 Lisbon, the M6.3 1909 Benavente, and M7.8 1969 Algarve. The country is characterized by holding an important proportion of unreinforced masonry buildings (URM), which is around 50 % according to the national institute of statistics [1]. Limestone, granite, schist and basalt are the most common stone types employed for building construction, in addition masonry buildings are mainly concentrated in the city centres and outside the cities. These buildings were constructed continuously in time, Fig. 1 shows the distribution of masonry building by construction period and number of storeys in percentage. An accentuated construction of masonry buildings is found between 20's and 80's for 2-storey and between 40's and 80's for 3-storey masonry buildings.

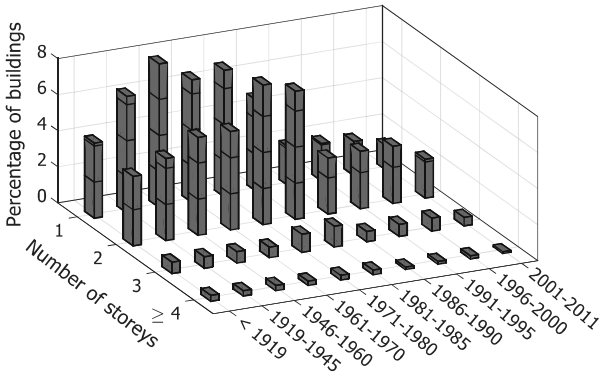

Fig. 1 – Distribution of masonry buildings per construction period and number of storeys (INE [1])

Masonry buildings are specially affected by seismic events, which has demonstrated its poor seismic performance worldwide. This behaviour is attributed to some aspects of masonry constructions like its massiveness, the low tensile strength, the poor connexion between elements, lack of maintenance, non-engineered design, and degradation due to weathering. In addition, the vast diversity of masonry assemblies, materials and building configurations leads to a large uncertainty, which this work aims at partially assess.

Record-to-record, together with building-to-building variability suppose the two sources of uncertainty referred by many authors [2-4]. [2] suggest to interpret building-to-building variability as intra and inter-building variability. Intra-building variability is associated to uncertainties within each specific building like mechanical properties, modelling strategy and analysis method, while inter-building variability is related to differences between single buildings. The herein proposed study focus in assessing building-to-building and record-to-record variability considering a set of randomly sampled building and a set of records as source of uncertainties. Analysis of uncertainties related to mechanical properties and modelling strategy can be found in [5] and [6] respectively.

Limestone 3-storey buildings were selected as case of study due to availability of data and to keep computational effort feasible. Probability density functions developed in Lovon et al. [7] are employed for building sampling. An advanced modelling technique is implemented thanks to Ls-Dyna [8,9] contact modelling capabilities, allowing to employ two novel engineering demand parameters (EDPs) in the analytical fragility assessment. Finally, cloud analysis [10] is used for fragility analysis fatality vulnerability functions are calculated with basis on the empirical relationships found in Abeling & Ingham [11].

2. Buildings Sampling

The characterization of limestone masonry buildings has been widely studied in Lovon et al. [7]. Table 2 shows geometric features applicable for 3-storey limestone masonry buildings together with probability density functions for random sampling.

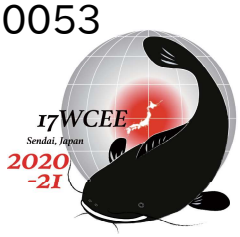

Table 1 – Geometric features for limestone and granite masonry buildings

Random variables	Unit	Limestone			Granite		
		Function	Mean	Std. deviation	Function	Mean	Std. deviation
Ground floor height	m	Normal	2.98	0.46	Normal	3.60	0.39
Upper storeys height	m	Normal	2.90	0.31	Normal	3.30	0.39
Length X-direction	m	Lognormal	6.70	2.70	Lognormal	6.20	0.94
Length Y-direction	m	Normal	8.20	2.10	Normal	17.0	3.90
Wall thickness (≤3 storeys)	m	Weibull	0.66	0.07	Weibull	0.54	0.11
Average wall thickness reduction	-	Gamma	0.15	0.09	Gamma	0.16	0.08
Opening ratio (ground)	-	Beta	0.46	0.14	Beta	0.55	0.13
Opening ratio (upper storeys)	-	Beta	0.27	0.05	Beta	0.43	0.10
Non-structural walls density	-	Gamma	0.026	0.010	Gamma	0.026	0.010

Limestone masonry archetypes were identified through revision of field data. It was found that number of openings (i.e. doors and windows) is related to the opening ratio, thus a set of archetypes were assigned to each range of openings area. Fig. 2 show the aforementioned arrangement, which represent a key step in the procedure of random sampling. Two to four rows of openings are assigned according to the range of area of openings, openings in the ground floor are assumed to be a combination of a window with a certain number of doors, while upper storeys may contain either windows or doors.

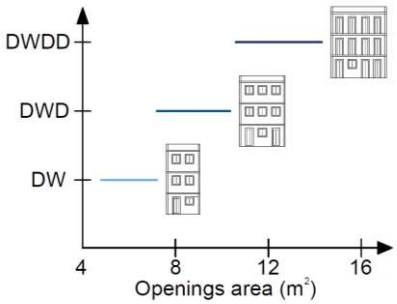

Fig. 2 – Openings area – archetypes association

Sampling procedure was conducted using Montecarlo simulation in MatLab software [12], a routine was implemented for this purpose. The procedure consists in using the probability density functions shown in Table 1 to sample an openings area, then an archetype is selected according to Fig. 2. The sizes of the openings were proposed to be from 0.8x1.8 (length x height) to 1.8x2.2 m for doors, and from 0.6x0.6 to 1.2x1.0 m for windows. The algorithm selects the size that best match the area of opening, residuals from the selection are minimum. A set of 20 buildings were sampled in order to consider the building-to-building variability in the fragility assessment procedure

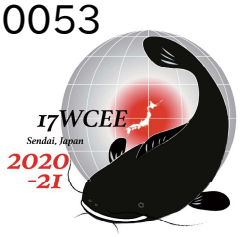

3. Structural Analysis

3.1 Numerical modelling

Numerical modelling has reported a significant advance in the last decades [13]. However, most of the approaches devoted to seismic assessment of masonry buildings are intended to assess near-collapse states. The modelling strategy herein employed has the intention to model the crack formation and collapse mechanism, thus leading to a clearer damage quantification for masonry buildings. The modelling strategy can be named as block-based according to the D'altri classification [13].

A set of elastic-behaviour blocks are attached through zero-thickness cohesive elements to represent the building. The non-linear behaviour concentrates in the joints, and blocks are released by deleting the cohesive elements. The *MAT_COHESIVE_MIXED_MODE material was selected for the cohesive elements; it has a linear behaviour followed by a linear softening. Fig. 3 illustrated the behaviour of cohesive elements and Eq. 1 shows its failure surface equation:

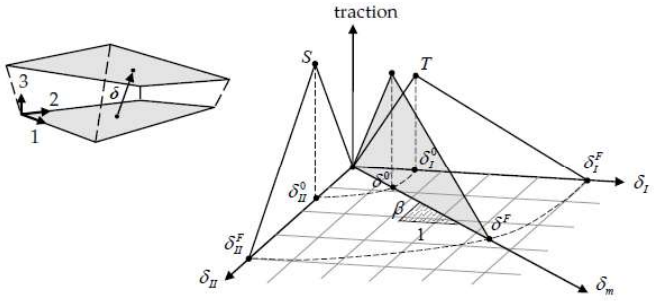

Fig. 3 – Mixed-mode force-separation law for cohesive elements [9].

$$\left(\frac{\sigma_n}{NFLS}\right)^2+\left(\frac{\sigma_s}{SFLS}\right)^2\geq 1 \tag{1}$$

where σ_n and σ_s are the shear and tensile stress in the interface, NFLS and SFLS are the shear and tensile maximum strength. The treatment for the interaction between blocks after the deletion of cohesive elements is solved through a penalty stiffness formulation implemented in Ls-Dyna software [9]. In short terms, it consists in allocating a spring in the nodes belonging to the master segment and slave node that are known to be in contact. The stiffness of the spring is calculated with basis in the bulk modulus, the area of the invaded face, the volume of the element in contact and the penalty stiffness factor. The latter parameter can be calibrated for different phenomena and material, and is herein adopted as 1, which is the default value posed in Ls-Dyna. Further information regarding penalty stiffness formulation can be found in [14]. Tangential contact is modelled with a Coulomb formulation with 0.6 and 0.8 dynamic and static friction coefficients. The model's solution is implemented in an explicit time-integration since the search of contact should be performed in short spans of time.

Roof modelling consist in a set of springs spaced each 40 cm can be loaded only in compression. The maximum compression strength is calculated considering a flexural-compression load with constant gravity. Timbered roof is one of the main systems used in masonry buildings in Portugal.

Mechanical properties for masonry buildings herein employed are shown in Table 2. These values were defined with basis in the characterization procedure performed in Lovon et al. [7], and have the intention to represent average values for the building class.

The interaction between debris and ground was not modelled since it increases the computational effort unnecessarily, thus a deletion criterion for elements falling below level zero was implemented. In addition, an Hourglass stiffness-based formulation was used in order to avoid hourglass effect in blocks, Belytschko approach with a 0.05 factor was selected.

Table 2 – Mechanical properties adopted for 3-storey limestone masonry buildings

Element	Description	Unit	Value
Solid Elements	Elasticity modulus	GPa	0.76
	Poison ratio	-	0.30
	Static coefficient of friction	-	0.30
	Dynamic coefficient of friction	-	0.20
Cohesive elements	Normal and shear failure stress	MPa	0.12
	Normal and shear energy release rate	N/m	25.00
	Normal and tangential stiffness	GPa	0.76
Springs	Timber elasticity modulus	GPa	7.00
	Timber elasticity modulus (5%)	GPa	4.70
	Design compressive strength	MPa	16.00
	Design bending strength	MPa	14.00

Due to the large number of elements and its devious configuration, an algorithm was made in MatLab software to automatically generate the input for Ls-Dyna. The algorithm emulates the interlocking effect by shifting parts in the horizontal plane. A building example with parts texture is shown in Fig. 4.

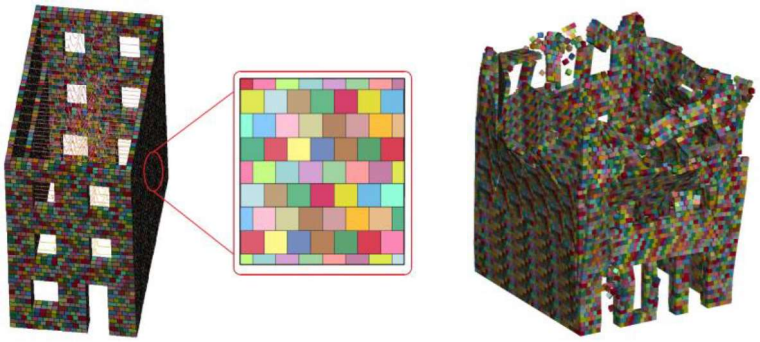

a) b)

Fig. 4 – a) Building example automatically generated and parts texture showing interlocking, b) Global instability of 3-storey masonry buildings, nonlinear time-history analysis.

3.2 Seismic demand

The hazard demand was represented by a set of 30 records with PGAs ranging between 0.05 to 0.95 g. This range was divided into 5 bins and records were scaled to cover at 6 records per bin because of the lack of historical data with high intensities. Fig. 5 shows the elastic response spectrum for a 5 % of critical damping in X and Y direction, being X aligned with the façade and Y perpendicular in the horizontal plane.

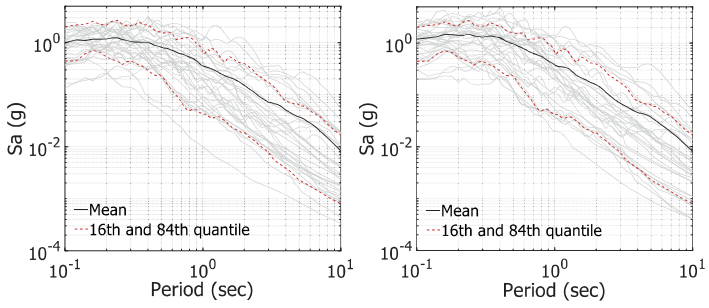

a) b)

Fig. 5 – Response spectrums for a) X and b) Y direction

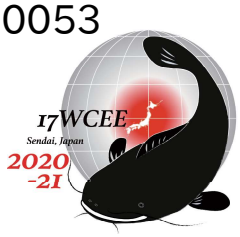

3.3 Damage threshold

Damage thresholds were defined with basis on two EDPs: crack propagation level and loss volume ratio. Crack propagation level is calculated as the quotient between the number of deleted and the total number of cohesive elements, and volume loss ratio is assessed as the ratio between debris and original volumes, thus EDPs configure constrained values between 0 and 1. Since slighter damage states are characterized by crack propagation across the building, thus their threshold is defined in terms of crack propagation level. Most extreme damage states are defined by volume loss ratio. Table 3 shows the damage threshold herein employed

Table 3 – Damage threshold

Damage state	EDP	Value
DS1 – negligible to slight	Crack propagation level	0.15
DS2 – moderate		0.25
DS3 – substantial to heavy	Volume loss ratio	0.10
DS4 – very heavy damage		0.25
DS5 – destruction		0.40

A third algorithm was implemented for output data collection, it is implemented in MatLab and advocated to print a set of instructions for Ls-prepost [15] software, the post-processing package of Ls-Dyna. Its capacity to represent the non-uniform distribution of damage, and to take into account mixed collapse mechanisms are most important advantages of the herein showed EDPs.

4. Uncertainties in physical damage fragility

Different procedures are proposed to calculate analytical fragility functions, however some of them require a large computational effort due to the need of performing subsequent analysis with scaled records. Cloud analysis [5,6,11] has been progressively employed for fragility analysis because its low demand of computational effort, and its versatility to model broad kind of uncertainties such as record-to-record, mechanical material properties and component capacity [3,5,6,16].

The cloud analysis can be defined as a linear regression-based probability model involving non-linear dynamic outputs. The first step consists in finding the best linear fit IM-EDP in the log space, homogeneity of variance is assumed around the best fit. Eq. 2 and 3 shows the probabilistic model:

$$E\left[\log(EDP)\middle|IM\right]=\log(a)+b\log(IM) \tag{2}$$

$$\sigma_{\log(EDP)|IM}=\sqrt{\frac{\sum_{i=1}^{n}\left(\log(EDP_i)-E\left[\log(EDP)\middle|IM_i\right]\right)^2}{n-2}} \tag{3}$$

Where $E[\log(EDP)|IM]$ stands for the expected logarithm of EDP given an IM, $\log(a)$ and b are the regression parameters, $\sigma_{\log(EDP)|IM}$ is the logarithmic standard deviation for the EDP given the IM, EDP_i corresponds to the $i-EDP$ value obtained from the non-linear analysis. The structural fragility obtained from the probabilistic model can be expressed as Eq. 4:

$$P\left[EDP \geq ds_i \middle| IM\right] = 1 - \Phi\left(\frac{\log\left(EDP_{dsi}\right) - E\left[\log\left(EDP \middle| IM\right)\right]}{\sigma_{total}}\right) \quad (4)$$

Where Φ is the cumulative normal standard distribution, EDP_{dsi} is the EDP damage threshold, and σ_{total} represent the total variability resulting from the building-to-building and record-to-record variability according to Eq. 5:

$$\sigma_{total} = \sqrt{\sigma_{btb}^2 + \sigma_{rtr}^2} \quad (2)$$

Fig. 6 illustrates the procedure above mentioned, the best fit is shown in blue line together with three IMLs in log scale and the corresponding probability of exceedance *Pe*. Then, the exceedance probabilities are plotted together with the IMLs in natural scale

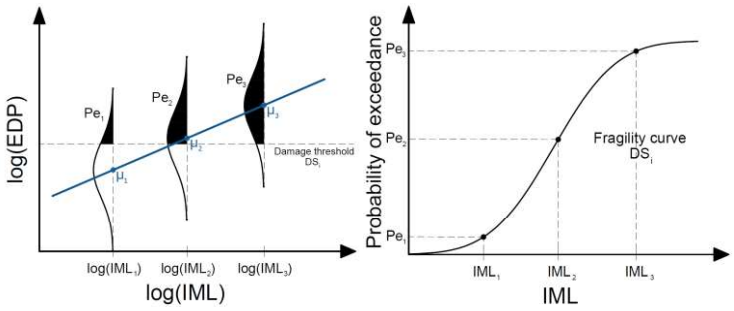

Fig. 6 – Steps of fragility assessment procedure a) probability of exceedance for 3 IMLs in i-damage threshold, b) Probability of exceedance – IMLs plot (fragility function) for i-damage state

The assessment of uncertainties associated to building-to-building and record-to-record was performed following three steps:

a) Each building results were processed using cloud analysis individually, thus it leads to the assessment of the record-to-record variability for the i-building, σ_{rtr-i}. The average σ_{rtr-i} is considered to represent the record-to-record variability for the building class, σ_{rtr}.

b) Cloud analysis was performed for all data in order to calculate the total variability σ_{total}.

c) The building to building σ_{btb} variability is calculated using Eq. 2.

Fig. 7 shows the results obtained after testing each building sampled in section 2 against each record selected in record 3.2.

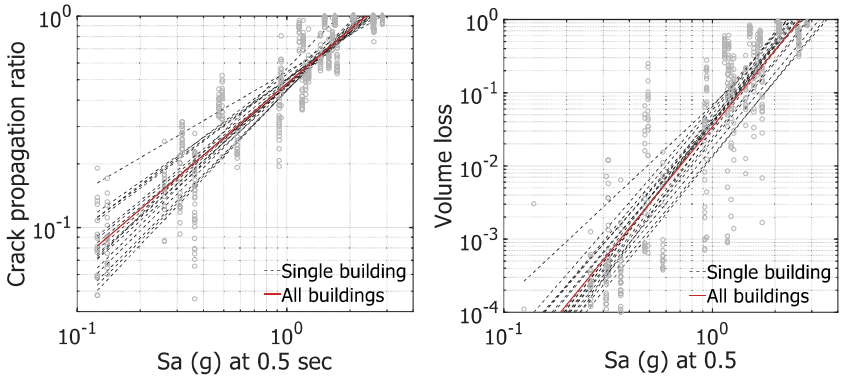

Fig. 7 – Best linear fit for a) Crack propagation level and b) volume loss. Red-dashed line is the best fit for the overall data, while black-continuous line is the best fit for each building

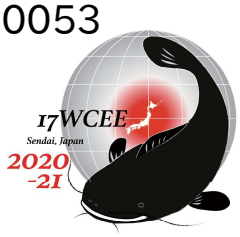

Dispersion parameters associated to the building-to-building and record-to-record are shown in Table 4. It should be noticed that building-to-building variability represent a significant source of the total uncertainty when using crack level propagation, however it is significantly less for volume loss ratio. Fragility functions for the studied building class are shown in Fig 8.

Table 4 – Uncertainty parameters for 3-storey limestone building class

EDP	σ_{rtr}	σ_{btb}	σ_{total}
Crack propagation level	0.30	0.12	0.32
Volume loss ratio	1.20	0.66	1.37

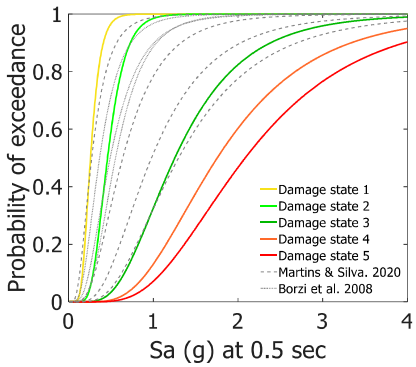

Fig. 8 – Fragility functions for 3-storey limestone masonry buildings.

Parameters of the fragility functions herein developed are shown in Table 5 for reproducibility. Damage states were defined with basis in the EMS-98 damage description, and values for damage threshold are proposed according to post-earthquake damage assessment data gathered by So [17].

Table 4 – Fragility functions parameters

Parameter	Negligible to slight	Moderate	Substantial to heavy	Destruction	Very heavy damage
μ	-1.35	-0.78	-0.23	0.56	0.73
σ	0.36	0.36	0.50	0.50	0.50

5. Fatality vulnerability assessment

The procedure herein employed aims at estimating fatality ratios induced by buildings collapse, which are cause of approximately 75 % of the fatalities due to earthquakes [18]. Commonly analytical vulnerability assessment is based in the assumption of strong correlation between physical damage and human losses [19,20]. However, it has been demonstrated by Okada [21] that most extreme damage states (DS) do not disclosure the level of destruction ([19, 22]). Thus existing damaged buildings classified in the same DS, but with different volume of debris. Lilian et al. [23] propose a set of EDPs with enhanced capacity for fatality prediction based in post-earthquake data recognition, being some of them more appropriate for certain structural systems. Volume loss is herein adopted, due to the massiveness inherent of stone masonry buildings. This parameter is calculated as the quotient between volume of debris and survival space, Fig. 8 illustrates the assessment of volume loss. Survival space is defined as the two meters above the reference level in the full plan area.

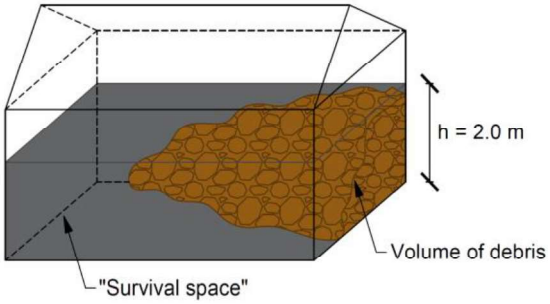

Fig. 9 – Volume loss (i.e. loss of survival space due to debris fall) adapted from [11].

Abeling et al. [11] propose a volume loss-fatality ratio correlation developed with field data of masonry damaged buildings. This relationship was used to calculate fatality ratios for volume loss outcomes from structural analysis described in section 3 leading to a fatality ratio-IML cloud of points. The set of points is then fitted to a log normal cumulative density function using least squares regression. Fig. 10 shows the best fit for each building and all data. Fig. 10 shows the fatality vulnerability functions herein obtained for 3-storey limestone masonry buildings together with other three approaches for comparison: a) The first approach uses physical damage fragility functions herein developed in and fatality ratios developed for cities in Europe [20] to assess fatality vulnerability functions, b) The second approach consists in using PAGER [24] empirical fatality ratios and Wald et al. [25] relationship convert the original IML (macro-seismic intensity) into PGA, then PGA values are transformed into Sa at 0.5 sec using average response spectrum factors.

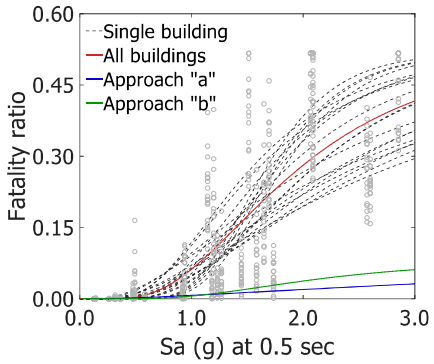

Fig. 10 – Fatality vulnerability functions.

6. Conclusions

A detailed numerical modelling strategy was implemented for structural assessment of masonry buildings. Due to the large effort that may demand the model setup, and output data collection, a set of algorithms were developed to automatize these procedures. This block-based approach, which has been employed previously for structural analysis of specific buildings, was now implemented for fragility and fatality vulnerability assessment of 3-storey limestone masonry buildings. Cloud method analysis was used for fragility analysis considering inter-building and record-to-record variability, and quantifying them. In addition, fatality vulnerability assessment was performed in the sampled building population leading to the conclusion that analysing a single building might bias the assessment of the building class. Future research should be conducted for other building classes in Portugal, and modelling uncertainties associated to the fatality vulnerability functions. The variability of building-to-building herein calculated serves to include this type of uncertainty in other classes.

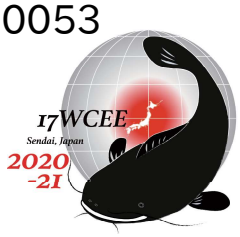

7. Acknowledgements

This study was supported by the Foundation for Science and technology (FCT) in the framework of the doctoral programme Infrarisk - Analysis and Mitigation of Risks in Infrastructures (PD/BD/150406/ 2019) and the research project PTDC/ECI-EST/31865/2017 MitRisk - Framework for seismic risk reduction resorting to cost-effective retrofitting solutions.

8. Copyrights

9. References

[1] I. N. de Estatística, "Census data 2011," Lisbon, 2011. [Online]. Available: http://censos.ine.pt/

[2] Silva V, Akkar S, Baker J, Bazzurro P, Castro J, Crowley H, Dolsek M, Galasso C, Lagomarsino S, Monteiro R, Perrone D, Pitilakis K, Vamvatsikos D (2019): Current chellenges and future trends in analytical fragility and vulnerability modelling. *Earthquake Spectra*, **35** (4), 1927-1952.

[3] Jalager F, De Risi R, Manfredi G (2015): Bayesian could analysis: efficient structural fragility assessment usinglinear regression. *Bulletin of Earthquake Engineering*, **13**, 1183-1203.

[4] Martins L, Silva V (2020): Development of a fragility and vulnerability model for global seismic risk analyses. *Bulletin of Earthquake Engineering*.

[5] Jalager F, Franchin P, Pinto PE (2017): A scalar damage measure for seismic reliability analysis of RC frames. *Earthquake Engineering and Structural Dynamics*, **36** (13), 2059-2079.

[6] Jalager F, Lervolino L, Manfredi G (2010): Structural modelling uncertainties and their influence on seismic assessment of existing RC structures. *Structural Safety*, **32** (3), 220-228.

[7] Lovon H, Silva V, Vicente R, Ferreira TM, Costa A (2021): Characterisation of the masonry building stock in Portugal for earthquake risk assessment. *Engineering Structures*.

[8] Hallquist J (2006): Livermore Software Technology Corporation. *Livermore Software Technology Corporation,* California.

[9] LSTC (2019): LS-DYNA keyword User's Manual. *Livermore Software Technology Corporation,* California.

[10] Jalager F (2014): Direct probabilistic seismic analysis: implementing Non-linear dynamic assessments. *PhD dissertation thesis University of Stanford*, California.

[11] Abeling S, Ingham J (2020): Volume loss fatality model for as-built and retroffited clay brick unreinforced masonry buildings damaged in the 2010/1 Canterbury earthquakes. *Structures*, **24**, 940-954.

[12] TM Inc (2018): MatLab. *Natick*, Massachusetts.

[13] D'Altri A, Sarhosis V, Milani G, Rots J, Cattari S, Lagomarsino S, Sacco E, Tralli A, Castellazzi G, Miranda S (2002): Modeling strategies for the computational analysis of unreinforced masonry structures: review and classification. *Archives of Computational Methods in Engineering*, **27**, 1153-1185.

[14] Huněk I (1993): On a penalty formulation for contact-impact problems. *Computers & Structures*, **48** (2), 193-203.

[15] LSTC (2019): LS-Pre/Post. *Livermore Software Technology Corporation,* California.

[16] Jalager F, Elefante L, Iervolino I, Manfredi G (2011): Knowledge-based performance assessment of existing RC buildings. *Journal of Earthquake Engineering*, **15** (3), 362-389.

[17] So E (2016): *Estimating fatality rates for earthquake loss models*. Springer, 1st edition.

[18] Coburn A, Spence R (2002): *Earthquake Protection*. John Wiley & Sons, 2nd edition.

[19] NIBS, FEMA (2013): HAZUS – MH 2.1 Earthquake model technical manual. *Technical Manual Washington D.C.: National Institute of Building Sciences (NIBS) and the Federal Emergency Management Agency*, Washington, USA.

[20] Spence R (2007): Earthquake disaster scenario predictions and loss modelling. *Lessloss – Risk mitigation for Earthquakes and Landslides*, Pavia, Italy.

[21] Okada S (1996): Description for indoor space damage degree of building in earthquake. *17th World Conference on Earthquake Engineering*, Acapulco, Mexico.

[22] ATC-13 (1985): Earthquake damage evaluation data for California. *Applied Technology Council*, California, USA.

[23] Iida A, Okada S, Nakashima T, Kitahara M (2017): Volumetric loss estimation for collapsed buildings during earthquakes. *16th World Conference on Earthquake Engineering*, Santiago, Chile.

[24] K. Jaiswal, D. J. Wald, and M. Hearne, "Estimating Casualties for Large Earthquakes Worldwide Using an Empirical Approach," 2009. doi: 10.3133/OFR20091136.

[25] D. J. Wald, V. Quitoriano, T. H. Heaton, and H. Kanamori, "Relationships between Peak Ground Acceleration, Peak Ground Velocity, and Modified Mercalli Intensity in California," Earthq. Spectra, vol. 15, no. 3, pp. 557–564, Aug. 1999, doi: 10.1193/1.1586058.

